ISSN 2176-5480

22nd International Congress of Mechanical Engineering (COBEM 2013)
November 3-7, 2013, Ribeirão Preto, SP, Brazil

NUMERICAL ANALYSIS OF ADHESIVE JOINTS BY THE FINITE ELEMENT METHOD CONSIDERING DAMAGE INITIATION AND EVOLUTION

Marçal Costa Samways
Roberto Dalledone Machado
Pontifícia Universidade Católica do Paraná. Rua Imaculada Conceição, 1155 Curitiba – Paraná. Brasil.
marcal.samways@pucpr.br; roberto.machado@pucpr.br

Abstract. *Nowadays, adhesive joints in structures are being used in several applications in engineering. This type of joints presents a major advantage in structural designs (high stiffness and very low density), resulting in components with a lower weight. The processes of damage on these types of materials tend to be very complex. For this reason, it becomes necessary to develop reliable methods to perform analyses on these components, in order to avoid damage and structural failures. The goal of this work is to study, analyze and compare the different techniques used in computer modeling of adhesive interfaces, considering the effect of the damage initiation and its evolution. Numerical models are reproduced in a commercial software, which is based on a finite element method (ABAQUS 6.10). Formulations of damage mechanics and its constitutive equations are considered in order to represent the correct behavior of the interface, and the verification of its resistance. To consider this mechanism of damage, the models that describe the damage initiation and evolution are evaluated in three different modes: Mode I, Mode II and Mixed-Mode Loading. The numerical results of these analyses are compared with results found in laboratorial and numerical tests available in the literature.*

Keywords: *Composite material, adhesive joint, cohesive element, damage initiation, traction separation.*

1. INTRODUCTION

Mechanical components united by the usage of adhesives are alternatives that are occurring with greater frequency in many structural applications. The characteristics of such unions makes them very attractive in industries such as aeronautics, automotive and civil/mechanical engineering. When comparing this method with conventional couplings by means of mechanical components (e.g. bolts, screws, etc.), it is noticed that the adhesive has the added benefit of generating less stress concentration, a more uniform load distribution and a better property for fatigue. Another advantage presented is the designs of structures with a lower self-weight. The usage of adhesive joints also makes possible the union between metallic surfaces with non-metallic surfaces, something unable by welding methods.

A type of component that uses adhesive joints is the composite material. A typical material of fiber reinforced composite consists of multiple layers of fibers adhered to each other. Composite materials are elements made of the same or different material type naturally designed (e.g. wood) or engineered (e.g. rolled plate). Generally, the failure process of these types of materials tends to be very complex, varying from intralaminar failures to interlaminar failures, the latter being known as delamination (Balzani and Wagner, 2008). Therefore, it is of paramount importance in this case the correct application of equations for the design of such materials because they are used in a vast range of engineering applications.

Given the increasingly usage of adhesive connections with important structural responsibility, it is required careful verification of such connections. According to Rudawska (2010), analytical methods for the determination of stresses on joints connected by adhesives have several simplifying considerations that make its final results unreliable. To avoid these difficulties, the Finite Element Method (FEM) is characterized as an excellent tool for computational analysis.

In the works of Camanho and D'Ávila (2002) and Xu *et al*. (2012), for the interface elements, a constitutive model called "traction-separation" is applied. In 1998, Geubelle and Baylor (1998) use this curve to simulate the initiation and propagation of cracks in composites formed by thin plates. Using such constitutive model, by increasing the separation of the interface, the stress along the adhesive reaches a maximum value (damage initiation) and, after this, this value decreases until a magnitude of zero, that being the point where the complete delamination (or complete damage) occurs. Thus, the focus of the work is to approach an analysis methodology for adhesive joints, taking into account the effects of damage to the interface elements.

2. MECHANICS OF THE DAMAGE

The strength of the bonded joints mainly depends on the behavior of the interface material. The literature shows that, with increased loadings, there is a tendency of damaging the adhesive material, which may compromise the strength and integrity of the connection. According to Lemaitre and Desmorat (2005), the damage is always related to the plasticity or irreversible deformations, and more generally also a dissipation of deformation. This process of evolution of the

ISSN 2176-5480

initial damage ultimately affects the elastic properties of the material or, better saying, a reduction of resistance and rigidity. Starting up to a more advanced stage of loading, the damage leads to the growth of microcracks too, creating a permanent deformation (Proença, 2000).

According to the definition of Lemaitre and Desmorat (2005), considering A_d as the damaged area and A as the undamaged area, the damage variable d is defined by the following relationship shown in Eq. (1).

$$d = \frac{\delta A_d}{\delta A} \tag{1}$$

Therefore, it can be seen that the range of possible values for the damage is from 0 to 1, where $d = 0$ corresponds to the material still intact and $d = 1$ refers to the moment where a state of complete damage is reached. The effective stress σ_{eff} in the case of an isotropic damage is defined by Eq. (2).

$$\sigma_{eff} = \frac{\sigma}{1 - d} \tag{2}$$

Thus, the basics of the damage in a component are presented. In summary, it can be said that the damage is the loss of rigidity of a structure according to any actual loss of area for the distribution of any applied force. Thus, it is possible to perform a compilation of the formulations involved in representing various types of interfaces. The emphasis in this case is given to elements used in the characterization of MZC.

3. FINITE ELEMENT – INTERFACE ELEMENTS

In the analyses of structural components where there is mutual interaction between two different bodies, the consideration of the interface region is of paramount importance for a correct evaluation of the stresses and strains that occur in this region. Many of the interface elements come from engineering studies for civil construction, which evaluates the interaction between soil/beam, concrete/beam or concrete/soil and so on. Such elements are used in conditions where two-dimensional approximation can be addressed. However, many interface elements allows their formulation to be used for the analysis of materials having adhesion functionality (adhesives or glues). These types of adhesions are characterized as Cohesive Zone Models (CZM), and the main differences are the introduction of the parameters of damage in its constitution, as well as the possibility of working with three-dimensional models. On the following section, some interface elements found in the literature are presented, as well as the CZM element used in this present work.

3.1 Interface Elements

As quoted by Lázaro (2004), in the study conducted by Ngo and Scordelis (1967), a finite element is created for its use in analysis of reinforced concrete beams. In the analyses performed, a three-dimensional beam is considered, composed of concrete and steel. As mentioned in the work of Kaliakin and Li (1995), Goodman *et al*. (1968) proposes an interface element for the analyses of rock masses. Ghabousi *et al*. (1973) propose a non-zero thickness element to represent connections between rocks and, thirty years later, Coutinho et al. (2003) describes an extension of the interface element proposed by Hermann (1978).

It should be emphasized that, on the elements briefly described above, all applications are only for two-dimensional cases. For the interface elements that are used to describe the cohesion between two surfaces, a state of tridimensional stresses occurs generally, making it necessary to characterize the existing damage in the element of adhesion. Cohesive Zone Models (CZM) are developed exclusively for application in regions which are joined by the means of an adhesive resin, being that for structural components joints or also for interlaminar fibers in a composite material. These CZM models are discussed in the following section.

3.2 Cohesive Zone Models (CZM)

Interface regions have been modeled in several different ways throughout recent history. The key to determine the best way of characterizing these interfaces is to use an approximation of the continuum mechanics, rather than the usage of simplifying forms of analysis, such as the use of springs in formulations of finite elements (Chandra *et al*., 2002). Recently, the usage of CZM has been widely used when it is desired to describe the initiation and propagation of damage in several different types of materials. The utilization of CZM in the modeling of interfaces presents distinct advantages compared with other methods, and this is based on micro-mechanical approaches.

The first CZM was developed by Barenblatt (1959) as an alternative to the concept of mechanical damage to fragile materials. Dugdale (1960) extended the concept created by Barenblatt (1959) for materials which are perfectly plastic to

ISSN 2176-5480

claim the existence of a processing zone at the base of existing cracks. According to Camanho and D'Àvila (2002), Needleman (1987) was the first researcher to use exponential functions and polynomial equations for interfaces analyses, in order to simulate the delamination in metallic materials. Tvergaard and Hutchinson (1992) analyze the growth of existing cracks and the corresponding strength of the cohesive element. Camacho and Ortiz (1996) describe in their work a Lagrangian finite element to analyze the fracture and fragmentation in brittle materials. Two years later, Geubelle and Baylor (1998) describe a bilinear model for the behavior of CZM. The emphasis of this present section is not to deepen and refine each CZM described, but to give a brief general history. However, in the following sections, the cohesion model described by Geubelle and Baylor (1998) is explained in detail. This is the CZM chosen to characterize the cohesive element in this present work. In section 3.2.1 it is presented the formulation of a solid cohesive element (with 8 nodes) and in section 3.2.2 the damage constitutive relation is described according to the Geubelle and Baylor (1998) CZM.

3.2.1 Cohesive Finite Element Formulation – Balzani and Wagner (2008)

In this section, the formulation of an interface element is described. The main focus is to use a continuum mechanics approach to the modeling of composite interlaminar damage. The formulation is based on an isoparametric element (solid element 8 nodes). It is considered a thin continuous element inserted between two plates, with a starting value of h_0 presenting a ratio of 1/100, with respect to the plate thickness (Balzani and Wagner, 2008). The remaining stresses on this element are the normal stresses σ_n (in the thickness direction), and the shear stresses τ_{sn} and τ_{tn} (in the directions transverse to the thickness), forming an interlaminar stress vector (Fig. 1).

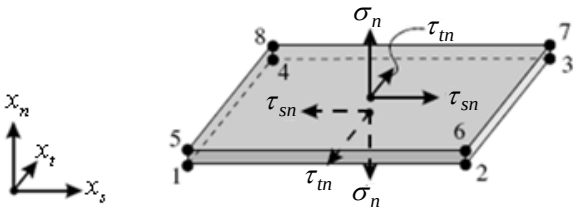

Figure 1. Tridimensional stress state of a solid interface element (Balzani and Wagner, 2008).

The interface element is referenced by a global rectangular coordinate system. In this system, the coordinates *s*, *t* and *n* are referent to the three vectors direction (x_S , x_t , x_n). The *n* vector is the direction of the adhesive thickness, and it corresponds to the mode I of failure (crack opening). The vectors *s* and *t* are the directions of the adhesive width and length, respectively, and corresponds to the mode II and III of failure (shearing on the transverse and parallel to the fiber).

Considering *V* as the element volume, according to the works of Balzani and Wagner (2008) and Kattan and Voyiadjis (2002), the principle of virtual work for solid interfaces can be described by the Eq. (3).

$$\delta \Pi(u) = \int_V [\,\delta\varepsilon^T\,][\,\sigma\,]\,dV \tag{3}$$

$\delta\varepsilon$ is the virtual strain vector and σ is the stress vector. The displacement vector u and the strain vector ε are defined by Balzani and Wagner (2008) by the Eq. 4. γ_{sn} and γ_{tn} represent the shear strain on the cross-sectional and longitudinal direction, respectively, and ε_n is the strain on the normal direction (adhesive thickness).

$$[\,u\,] = \begin{bmatrix} u_s \\ u_t \\ u_n \end{bmatrix},\ [\,\varepsilon\,] = \begin{bmatrix} \gamma_{sn} \\ \gamma_{tn} \\ \varepsilon_n \end{bmatrix} = \begin{bmatrix} u_{s,n} + u_{n,s} \\ u_{t,n} + u_{n,t} \\ u_{n,n} \end{bmatrix} \tag{4}$$

The symbol Δu represents the incremental displacement vector. Working on the Eq. (3), the Eq. (5) is obtained. On this Eq. (5), the parameter *C* is the constitutive behaviour of the material.

ISSN 2176-5480

$$\delta \Pi(u) = \int_V [\,\delta\varepsilon^T\,]\{\,C\,\}([\,\varepsilon\,] - [\,\varepsilon_0\,])dV = \int_V [\,\delta\varepsilon^T\,]\{\,\frac{\partial\sigma}{\partial\varepsilon}\,\}[\,\Delta\varepsilon\,]\,dV \tag{5}$$

When approaching the formulation from the point of view of the finite element concepts, a discretization is performed on the interface element. In this case, it is considered a shape function N_i with natural coordinates for an isoparametric 8 node element. The quantities ξ, χ and ν represents the directions on the natural coordinates. In the global coordinate, these directions are represented by x_n, x_s e x_t.

Adopting x as the nodal position vector, any node position can be obtained from Eq. (6). Therefore, the relationship between natural and global coordinates is defined as follows:

$$x(\xi,\chi,\nu) = \sum_{i=1}^{8}\{\,N_i\,\}x_i \tag{6}$$

Thus, the strains can be defined by Eq. (7), and the tensor B is described by Eq. (8).

$$\{\,\varepsilon\,\} = \sum_{i=1}^{8}\{\,B_i\,\}[\,u_i\,] \tag{7}$$

$$\{\,B_i\,\} = \begin{Bmatrix} \frac{\partial N_i}{\partial x_n} & 0 & \frac{\partial N_i}{\partial x_S} \\ 0 & \frac{\partial N_i}{\partial x_n} & \frac{\partial N_i}{\partial x_t} \\ 0 & 0 & \frac{\partial N_i}{\partial x_n} \end{Bmatrix} \tag{8}$$

Considering K^e_{Tik} as the element stiffness tangential matrix, the principle of virtual work can be described in the Eq. (9).

$$\Delta\delta\Pi = \sum_{i=1}^{8}\sum_{k=1}^{8}[\,\delta u_i^T\,]\int_V\{\,B_i^T\,\}\{\,C\,\}\{\,B_K\,\}dV\,[\,\Delta u_k\,] = \sum_{i=1}^{8}\sum_{k=1}^{8}[\,\delta u_i^T\,]\{\,K^e_{Tik}\,\}[\,\Delta u_k\,] \tag{9}$$

Therefore, Eq. (9) represents the principle of virtual work on the 8 node solid element. According to Balzani and Wagner (2008) and Camanho and D'Ávila (2002), the Newton-Cotes integration results in a better performance of the element. Inside Eq. (9) it is necessary the implementation of a constitutive relation which represents the damage on the interface element. On the following section, a constitutive equation (based on the Geubelle and Baylor (1998) CZM) proposed by Camanho and D'Ávila (2002) is presented.

3.2.2 Cohesive Finite Element Formulation – Camanho and D'Ávila (2002)

The need for an appropriate constitutive equation, in the formulation of the cohesive element, is due to the fact that this is critical for a proper evaluation of the entire process of damage on the interface. This section describes the proposed cohesive laws in a model described by Camanho and D'Ávila (2002). This model allows a prediction of the damage initiation and propagation under a loading application called "mixed-mode". Figure 2 shows the behavior of the material in this model. σ_n^0 and τ_S^0 are, respectively, the normal an shear maximum stresses capacities of the interface. The quantities u_n^0 and u_S^0 are, respectively, the displacements necessary to achieve the normal and shear maximum stresses (this is the damage initiation point). And, finally, u_n^f and u_S^f are, respectively, the final displacements necessary to achieve failure (total damage).

ISSN 2176-5480

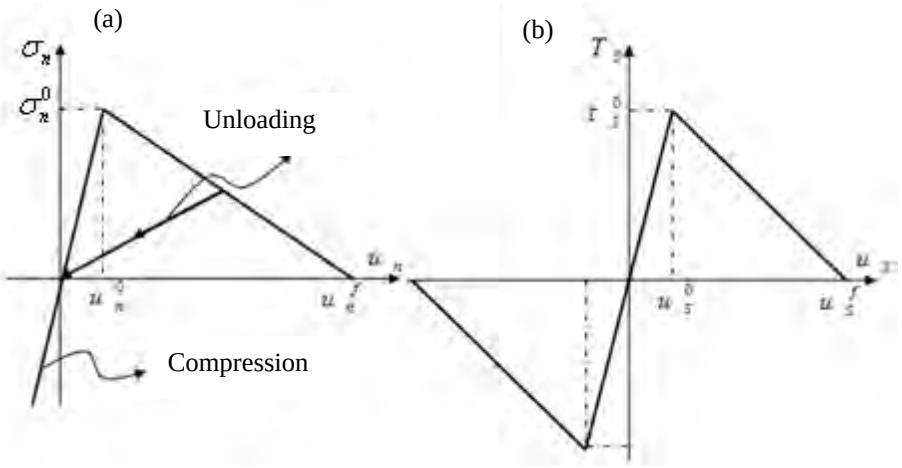

Figure 2. Damage bilinear model: (a) Mode I of loading; (b) Modes II and III of loading.

The property K (penalty stiffness) is one of the properties needed to define the actual behavior of the interface, being responsible for the elastic property of the element. Other properties are required for the same purpose, as the fracture energy ($\Gamma_N, \Gamma_S, \Gamma_t$). With the objective of obtaining a more complete formulation in the constitutive equations, Camanho and D'Ávila (2002) defines a behavior where there is also an unloading involved. In this case, the loading condition can be formulated as a function of a variable, called maximum relative displacement (u^{max}). Equation (10) demonstrates this internal variable that governs the maximum displacement computed.

$$u_i^{max} = max\{ u_i^{max}, |u_i| \}, i = s,t,n \tag{10}$$

Adopting in this case an *F* function to distinguish loading and unloading, described by Eq. (11). The term ‹ › refers to the "Macaulay Bracket".

$$F = \frac{\left\langle |u_i| - u_i^{max} \right\rangle}{|u_i| - u_i^{max}}, i = s,t,n \longrightarrow Mode\ I, II\ or\ III \tag{11}$$

The elasticity matrix *D*, which contains the cohesive properties inside the interface, is defined by the Eq. (12). The term I is the identity matrix.

$$D = \begin{cases} K\{I\} & \longrightarrow \quad u_i^{max} \le u_i^0 \\ (1-d)K\{I\} + dK\dfrac{\langle -u_n \rangle}{-u_n} & \longrightarrow \quad u_i^0 < u_i^{max} \le u_i^f \\ K\dfrac{\langle -u_n \rangle}{-u_n} & \longrightarrow \quad u_i^f \le u_i^f \end{cases} \tag{12}$$

The *d* scalar parameter, used for the calculation of the damage extension, is introduced on the Eq. (12) and, according to Camanho and D'Ávila (2002), this parameter is described by the Eq. (13).

$$d = \frac{u_i^f (u_i^{max} - u_i^0)}{u_i^{max} (u_i^f - u_i^0)} \tag{13}$$

Therefore, Balzani and Wagner (2008) obtain the stress linearization matrix, described by Eq. (14).

$$C = \{D\} + K\left(\frac{u_i^0 u_i^f}{(u_i^{max})\ (u_i^f - u_i^0)} \right) F(\{I_C\} - \{I\})(\varepsilon\varepsilon^T) \frac{\left\langle u_i - u_i^0 \right\rangle}{u_i - u_i^0} \frac{\left\langle u_i^f - u_i \right\rangle}{u_i^f - u_i} \tag{14}$$

ISSN 2176-5480

3.2.3 Damage Initiation and Propagation

In the works of Ghosh *et al.* (2000) and Chandra *et al.* (2002), the fracture energy Γ on the interface represents the area under the stress x relative displacement curve shown on Fig. 2, and its values are obtained by Eq. (15). According to Camanho and D'Ávila (2002), the displacement initial and final values are defined by the Eq. (16).

$$\Gamma_i = \int_0^{u_i^f} \sigma_i du_i = \frac{1}{2}\sigma_i u_i^f \tag{15}$$

$$u_i^0 = \frac{\sigma_i^0}{K};\ u_i^f = \frac{2\Gamma_i}{\sigma_i^0} \tag{16}$$

According to Camanho and D'Ávila (2002), the initial damage can be predicted by a quadratic failure criterion, defined by Eq. (17).

$$\left(\frac{\langle \sigma_N \rangle}{\sigma_n^0}\right)^2 + \left(\frac{\tau_S}{\tau_S^0}\right)^2 + \left(\frac{\tau_t}{\tau_t^0}\right)^2 = 1 \tag{17}$$

In the case of positive crack openings u_n, it is introduced a mixed-mode ratio β, defined by Eq. (18).

$$\beta = \frac{u_{cisalh}}{u_n} \tag{18}$$

Thus, the effective relative displacement on the mixed-mode loading on damage onset is defined by Eq. (19).

$$u_m^0 = \begin{cases} u_n^0 u_S^0 \sqrt{\dfrac{1+\beta^2}{(u_S^0)^2 + (\beta u_n^0)}} & \longrightarrow \quad u_n > 0 \\ u_{cisalh}^0 & \longrightarrow \quad u_n \le 0 \end{cases} \tag{19}$$

When mixed-load is observed, Camanho and D'Ávila (2002) recommends the B-K criteria, proposed at first by Benzehhagh and Kenane (1996). This criterion is defined by Eq. (20).

$$\Gamma_C = \Gamma_N + (\Gamma_S - \Gamma_N)\left(\frac{\Gamma_{II}}{\Gamma_T}\right)^{\eta},\ \textit{with}\ \Gamma_T = \Gamma_I + \Gamma_{II} \tag{20}$$

In Eq. (20), Γ_I and Γ_{II} are the modes I and II energy loss ratio, respectively, and Γ_C is the critical energy loss ratio on the mixed-mode loading. The total energy loss is defined by Γ_T. The η parameter is used to adapt the curve obtained experimentally (the "Least Square Fitting Method" is used in order to fit the points obtained experimentally into a curve). In this case, the value obtained by Camanho and D'Ávila (2002) for the η parameter is 2.284.

When submitted to mixed-mode loading, the energy loss ratios that correspond to the total failure displacements are defined by Eq. (21) and Eq. (22).

$$\Gamma_I = \frac{K u_m^{n\,f} u_m^{cisalh0}}{2} \tag{21}$$

$$\Gamma_{cisalh} = \frac{K u_m^{cisalh\,f} u_m^{cisalh0}}{2} \tag{22}$$

ISSN 2176-5480

In Eq. (21) and Eq. (22), u_m^{n0} and $u_m^{cisalh\,0}$ represent the initial relative displacements in the normal and shear direction, respectively. Similarly, the values of $u_m^{n\,f}$ and $u_m^{cisalh\,f}$ represent the final relative displacements in the normal and shear direction (point when the complete damage occurs), respectively, when the component in question is subjected to a mixed mode. These displacement values are obtained according to Eq. (23) and Eq. (24).

$$u_m^{n0} = \frac{u_m^0}{\sqrt{1+\beta^2}}, u_m^{n\,f} = \frac{u_m^f}{\sqrt{1+\beta^2}} \tag{23}$$

$$u_m^{cisalh\,0} = \frac{u_m^0}{\sqrt{1+\beta^2}}, u_m^{cisalh\,f} = \frac{u_m^f}{\sqrt{1+\beta^2}} \tag{24}$$

Thus, an expression in function of the fracture energies in mode I and II is obtained, in order to verify the effective displacement on the total damage in the mixed-mode. This formulation is presented in Eq. (25).

$$u_m^f = \begin{cases} \dfrac{2}{Ku_m^0}\left[\Gamma_N + (\Gamma_S - \Gamma_N)\left(\dfrac{\beta^2}{1+\beta^2}\right)^2\right] & \longrightarrow \quad u_n > 0 \\ \sqrt{(u_S^f)^2 + (u_t^f)^2} & \longrightarrow \quad u_n \le 0 \end{cases} \tag{25}$$

4. APLICATIONS

In this section, some analyses of a composite model are presented. In these analyses, all the theory and formulations mentioned in the previous sections are applied. The analyses are performed in commercial finite element based software (ABAQUS 6.10), using exactly the same values for the mechanical properties and geometry also adopted by Camanho and D'Ávila (2002) for the DCB (Double Cantilever Beam) test. The details of the numerical modeling are also presented, plus all the values used for a correct approach to the initiation and propagation of the damage. Finally, these numerical results are compared with the values obtained by Camanho and D'Àvila (2002), experimentally and numerically.

4.1 Numerical Analysis – Double Cantilever Beam Test (DCB)

In their work, Camanho and D'Ávila (2002) performed laboratorial tests on different types of specimens with different methods of loading application, in order to verify the delamination of a composite material (AS4/PEEK). Different types of loading are applied according to Benzeggagh and Kenane (1996), with the objective of studying the delamination under the action of loads in Mode I, Mode II and Mixed Mode loading. After obtaining experimental results, Camanho and D'Ávila (2002) performed numerical analysis using an interface cohesive element (8 nodes) able to deal with damage in the mixed mode loading condition. This element is inserted between the solid elements (representing the laminates) in order to model the initiation and propagation of damage in composites. Figure 3 shows the DCB specimen, at first designed by Reeder and Crews (1990), to verify the delamination in Mode I (crack opening). In this case, the force P is applied perpendicular to the face of adhesion between the two solids, generating a normal load surface.

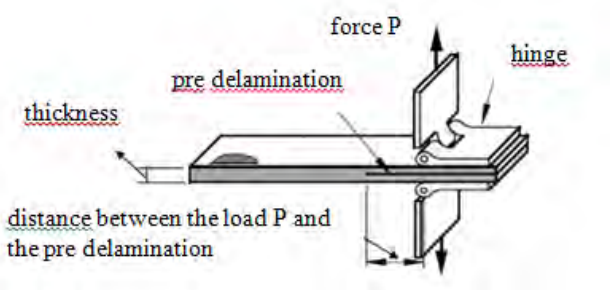

Figure 3. DCB testing apparatus (Reeder and Crews, 1990).

ISSN 2176-5480

This model has the same geometry of the specimen analyzed by Camanho and D'Ávila (2002), as well as the same mechanical properties. Figure 4 illustrates the modeling of the DCB specimen. Region 1 represents the region where damage can't propagate. Region 2 represents the location where the cohesive element is inserted between the two layers of the composite, this being the region responsible for identifying the beginning and propagation of the damage. Region 3 is where the pre-delamination (crack) is introduced into the specimen. According to Balzani and Wagner (2008), the initial value for the interface element height is sufficiently represented by the relation $h_0 = 2h / 100$ (h =1.56 mm). Thus, in this case the initial height of the cohesive element is 0.032 mm. The image presented in Fig. 5 shows the boundary conditions applied on the model.

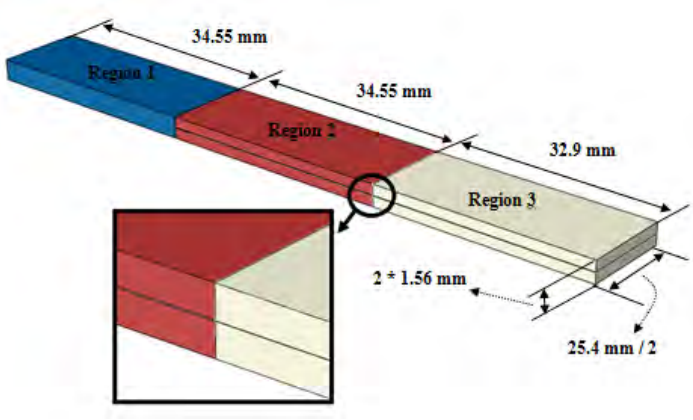

Figure 4 –DCB numerical model.

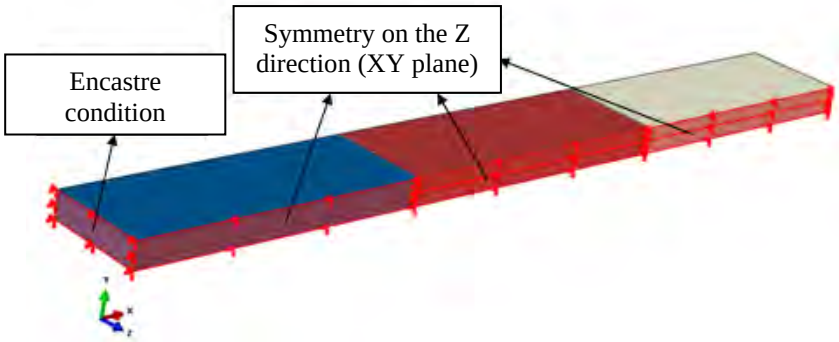

Figure 5. Boundary condition applied on the model.

Figure 6 shows the points where the displacements are imposed. These points, both at the top and the bottom of the model, are the regions where the reaction force P is observed throughout the history of the analysis. Initially, for a first analysis, the Z distance illustrated in Figure 8 has a value of 0.75 mm. Afterwards, this distance is changed at first to 1.50 mm and, in a third analysis, to 2.25 mm in order to verify the influence of this parameter on the results obtained.

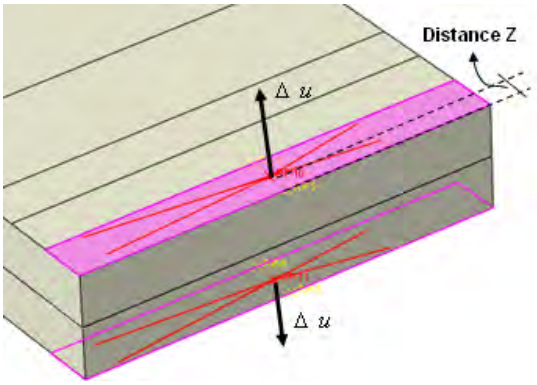

Figure 6. Displacement imposed on the points located at the "Distance Z".

ISSN 2176-5480

The generated mesh in the solid body representing the laminate itself is formed by elements with 8 nodes with a linear formulation. As for the cohesive element, located in Region 2 between the laminates, the mesh is formed by 8 nodes cohesive elements, also with a linear formulation. On Fig. 7, it is possible to verify the mesh generated on the cohesive element.

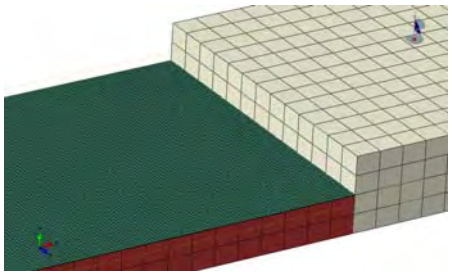

Figure 7. Mesh generated on the cohesive element.

In Tab. 1 it is shown the inter and intralaminar mechanical properties of the material used for the AS4/PEEK (APC2), a composite reinforced by carbon fibers (Reeder and Crews, 1990). The parameter *K*, in this case, has a value of 10E6 N/mm^3.

Table 1. Mechanical Properties of the composite AS4/PEEK (APC2).

E_{11} (GPa)	$E_{22}=E_{33}$(GPa)	$G_{12}=G_{13}$(GPa)	G_{23} (GPa)	$\mu_{12}=\mu_{13}$
122.7	10.1	5.5	3.7	0.25
μ_{23}	Γ_N (N/mm)	Γ_S (N/mm)	σ_N^0 (Mpa)	τ_S^0 (Mpa)
0.45	0.969	1.719	80	100

In the next step, the results obtained are shown. The values are compared to the ones obtained experimentally and numerically by Camanho and D'Ávila (2002). Figure 8 shows the curves (Force [N] x Displacement [mm]) generated on the first analysis, considering the distance Z (Fig. 6) with 0.75 mm. Figures 9 and 10 shows the curves generated considering the same distance Z with 1.50 mm and 2.25 mm, respectively.

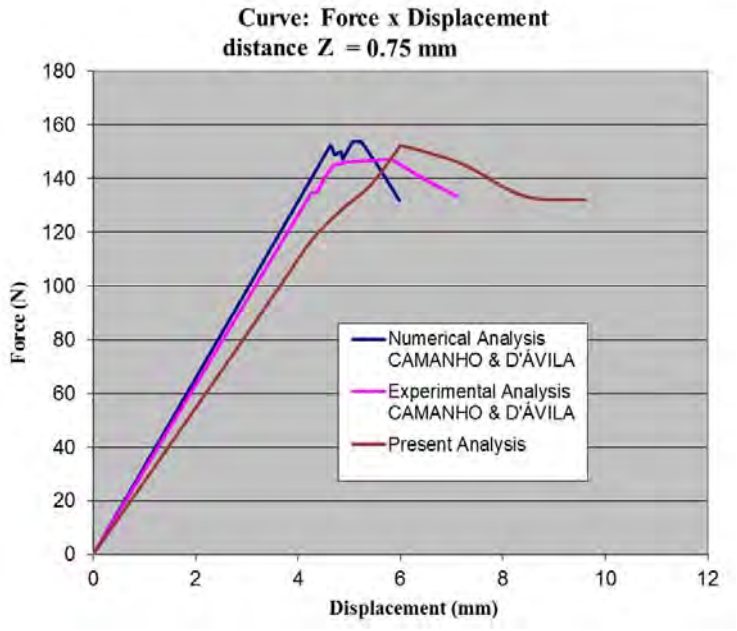

Figure 8. Curve: Force x Displacement – distance Z = 0.75 mm.

ISSN 2176-5480

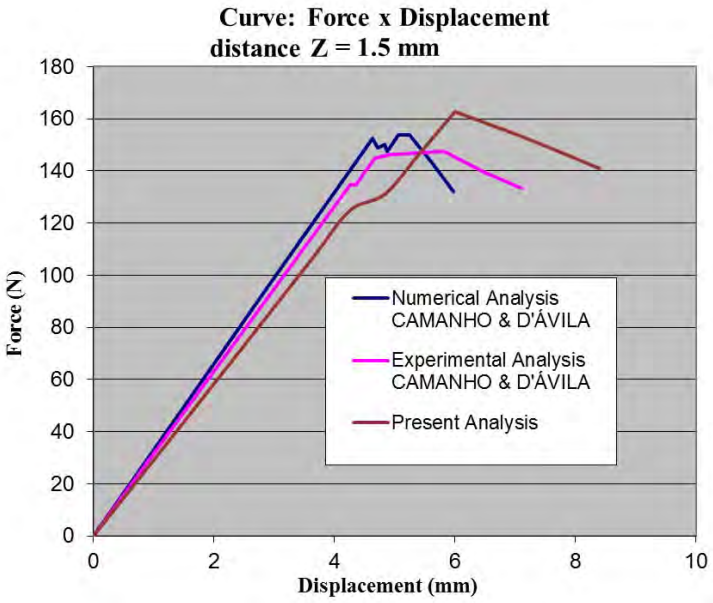

Figure 9. Curve: Force x Displacement – distance Z = 1.50 mm.

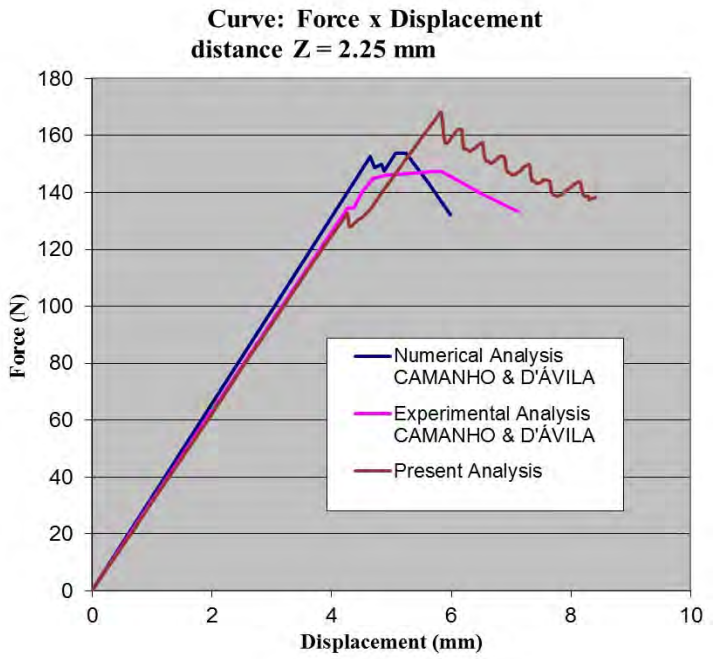

Figure 10. Curve: Force x Displacement – distance Z = 2.25 mm.

The values obtained for each configuration of the distance Z are shown on Tab. 2, 3 and 4. The maximum P force is presented with the correspondent relative error as well, comparing these values with the ones obtained by Camanho and D'Ávila (2002).

Table 2- Relative errors obtained for the distance Z=0.75mm.

$P_{máx}$ experimental (Camanho and D'Ávila, 2002)	$P_{máx}$ numérical (Camanho and D'Ávila, 2002)	$P_{máx}$ numerical (present analisis)	Relative error ($P_{máx}$ experimental)	Relative Error ($P_{máx}$ numérical)
147.11 N	153.27 N	152.50 N	3.66 %	0.5 %

ISSN 2176-5480

Table 3- Relative errors obtained for the distance Z=1.50mm.

$P_{máx}$ experimental (Camanho and D'Ávila, 2002)	$P_{máx}$ numérical (Camanho and D'Ávila, 2002)	$P_{máx}$ numérical (present analisis)	Relative error ($P_{máx}$ experimental)	Relative Error ($P_{máx}$ numérical)
147.11 N	153.27 N	162.66 N	10.57 %	6.12 %

Table 4- Relative errors obtained for the distance Z=2.25mm.

$P_{máx}$ experimental (Camanho and D'Ávila, 2002)	$P_{máx}$ numérical (Camanho and D'Ávila, 2002)	$P_{máx}$ numérical (present analisis)	Relative error ($P_{máx}$ experimental)	Relative Error ($P_{máx}$ numérical)
147.11 N	153.27 N	168.34 N	14.43 %	9.83 %

The results obtained shows that the change on the distance Z does have a significant impact on the behavior of the DCB test apparatus, when submitted to a mode I loading condition. Although the results for the configuration of Z=0.75 mm shows a low relative error (Tab. 2), the curve for the same configuration (Fig. 8) shows that the elastic behavior does not comply with the curve obtained by the refence. As the distance Z increases, it is observed that the curve generated (Fig. 9 and 10) tends to get more and more similar to the one obtained by this reference.

In general, it can be stated that the results presented above shows that the numerical analysis of the DCB apparatus performed in this work generates results very close to those obtained by Camanho and D'Ávila (2002).

5. CONCLUSIONS

In engineering designs, where adhesive resins are used as the method of joining components, it is necessary to take into account numerical methods and computational models which best correspond with the reality, both from the standpoint of the quality of the final product as by their safety as well. Accordingly, it is justifiable to search for efficient and reliable methods that make possible the evaluation of components that has bonded faces. For this reason, this paper seeks a better way to implement the FEM using the "traction-separation" law to represent the behaviour of damage in cohesive elements.

In computational analyses performed (ABAQUS 6.10) for composite materials, where the laminated layers are bonded together by the means of an adhesive resin, it is clear that the behaviour of these adhesives are very similar to the results found in the literature (Camanho and D'Ávila, 2002). However, in the case of the DCB testing apparatus, the exact location where the application of the displacement proved to be critical to obtain a more accurate result. Unfortunately, this information is not present on the reference adopted. The lack of accuracy in applying this parameter makes it very difficult to the convergence and leads to results that do not correspond 100% to the results obtained experimentally and numerically by Camanho and D'Ávila (2002), although the errors found are considered to be low.

The penalty stiffness K of the cohesion elements used appears to be a value very difficult to obtain, both in laboratorial tests or by analytical methods. It is unanimous among the references used that the values assigned to that property must have extremely high magnitude and the value of 10E6 N/mm3 is generally used in the analyses. The value adopted led to good results in computational analyses performed in this study and, therefore, it can be said that it is a consistent way to represent the elastic property of the adhesive with K=10E6 N/mm^3 in other analyses of cohesive interfaces.

Therefore, the results presented in this study proves that the usage of the Finite Element Method using commercial software, in this case ABAQUS 6.10, produces very similar results to those obtained in experimental and numerical tests available in the literature. The use of this tool in the analysis of adhesive materials leads to knowledge of what are the most important parameters to be considered for engineering projects.

6. REFERENCES

ABAQUS 6.10/ User's Manual Dassault Systems Simulia Corp., Providence, RI, USA.

Balzani, C. and Wagner, W., 2008. "An interface element for the simulation of delamination in unidirectional fiber-reinforced composite laminates". Engineering Fracture Mechanics, 75, 2597–2615.

Barenblatt, G.I., 1959. "The formation of equilibrium cracks during brittle fracture. General ideas and hypothesis. Axially-symmetric cracks". Prikladnaya Matematika i Mekhanika, 23, 434-444.

Benzeggagh, M.L. and Kenane, M., 1996. “Measurement of Mixed-Mode Delamination Fracture Toughness of Unidirectional Glass/Epoxy Composites with Mixed-Mode Bending Apparatus”. Composites Science and Technology, 56, 439-449.
Camacho, G.T. and Ortiz, M., 1996. “Computational modeling of impact damage in brittle materials”. International Journal of Solids and Structures, 33, 2899-2938.
Camanho, P.P. and D’Ávila, C.G., 2002. “Mixed-mode decohesion finite elements for the simulation of delamination in composite materials”. NASA Report-No. TM-2002-211737.
Chandra, N., Li, H., Shet, C. and Ghonem, H., 2002. “Some issues in the application of cohesive zone models for metal-ceramic interfaces”. International Journal of Solids and Structures, 39,2827-2855.
Coutinho, A.L., Martins, M.A., Sydenstricker, R.M., Alves, J.L. and Landau, L., 2003. “Simple zero thickness kinematically consistent interface elements”. Computers and Geotechnics, 30, 347-374.
Dugdale, D.S., 1960. “Yielding of steel sheets containing slits”. Journal of the Mechanics and Physics of Solids, 8, 100-104.
Geubelle, P.H., Baylor, J., 1998. “Impact-induced delamination of laminated composite: a 2D simulation”. Composites Part B, 29, 589-602.
Ghabousi, J., Wilson, E.L. and Isenberg, J., 1973. “Finite element for rocks joints and interfaces”. Journal of the Soil Mechanics and Foundations Division, 99, 833-848.
Ghosh, S., Ling, Y., Majumdar, B. and Kim, R., 2000. “Interfacial debonding analysis in multiple fiber reinforced composites”. Mechanics of Materials, 32, 561-591.
Goodman, R.E., Taylor, R.L. and Brekke, T.L.A., 1968. “A model for the mechanics of jointed rock”. Journal of the Soil Mechanics and Foundations Division, 94, 637-659.
Hemrann, L.R., 1978. “Finite element analysis of contact problems”. Journal of the Soil and Mechanics Foundation Division, 104, 1043-1059.
Kaliakin, V.N. and Li, J., 1995. “Insight into deficiences associated with commonly used zero-thickness interface elements”. Computers and Geotechnics, 17, 225-252.
Kattan, P. and Voyiadjis, G., 2002. “Damage Mechanics with Finite Elements – Practical Applications with Computational Tools”. Springer, Berlin, 1st edition.
Lázaro, F.P., 2004. “Análise não-linear da interação solo-duto em encostas empregando elementos de interface”, Master Degree Dissertation, Departamento de Engenharia Civil, Rio de Janeiro, Brazil.
Lemaitre, J. and Desmorat, R., 2005. “Engineering Damage Mechanics – Dutile, creep, fatigue and brittle failures”. Springer, Heilderberg 1st edition.
Neeleman, A., 1987. “A continuum model for void nucleation by inclusion debonding”. Journal of Applied Mechanics, 54, 525-531.
Ngo, D. and Scordelis, C., 1967. “Finite Element Analysis of reinforced concrete beams”. Journal American Concrete Institute, 64,152-163.
Proença, S., 2000. “Introdução à Mecânica do Dano e Fraturamento - Elementos de Mecânica do Dano em Meios Contínuos”. Text nº4, São Carlos, Brazil.
Reeder, J.R. and Crews J.H., 1990. “Mixed-mode Bending Apparatus for Delamination Testing”. AIAA Journal, 28, 1270-1276.
Rudawska, A., 2010. “Adhesive joint strength of hybrid assemblies: Titanium sheet- composites and aluminium sheet-composites-Experimental and numerical verification”. International Journal of Adhesives, 30,574–82.
Tvergaard, V. and Hutchinson, J.W., 1992. “The relation between crack growth resistance and fracture process parameters in elastic-plastic solids”. Journal of the Mechanics and Physics of Solids, 40, 1377-1397.
Xu, W. and Wei Y., 2012. “Strength and interface failure mechanism of adhesive joints”. International.Journal of Adhesion and Adhesives, 34, 80–92.

7. RESPONSABILITY NOTICE

The authors are the only responsible for the printed material included in this paper.